Indian Journal of Chemistry
Vol. 60A, November 2021, pp. 1416-1426

Microwave synthesis, characterization and biological activities of transition metal complexes with novel SNSN donor Schiff base ligand

P R Sagunthala Devi[a], S Theodore David[a,]*, C Joel[b], R Biju Bennie[b] & S Daniel Abraham[c]

[a]Research Department of Chemistry, PSN College of Engineering and Technology, Tirunelveli 627152, Tamil Nadu, India

[b]Postgraduate Department of Chemistry, St. John's College, Tirunelveli 627002, Tamil Nadu, India

[c]Department of Chemistry, Madras Christian College, Chennai 600059, Tamil Nadu, India

*E-mail: s.theodore.david@gmail.com

Received 11 August 2021; revised and accepted 26 October 2021

A novel Schiff base *(E)-N*-(pyridine-2-yl)thiophen-2-ylmethylene)hydrazine carbothioamide (L), has been synthesised by the condensation of thiophen-2-carbaldehyde and 4-(pyridin-2-yl)-thiosemicarbazide, using solvent free microwave synthesis. The Co(II), Ni(II), Cu(II) and Zn(II) complexes of the Schiff base are also prepared. They are characterised by elemental analysis, EI-mass spectrum, ^{1}H &^{13}C-NMR spectrum, FTIR, UV-vis spectra, magnetic, EPR spectra and thermal analysis. The "*SNSN*" donor ligand binds the metal ion in tetradentate mode through thiophenyl and thioenolic sulphur atoms and imino and pyridine nitrogen atoms. The electronic spectra along with magnetic measurements demonstrate tetrahedral geometry for Co(II), Ni(II) and Zn(II) complexes, and square planar geometry for Cu(II) complex. All the complexes are found to be thermally stable from thermogravimetric studies. The complexes show enhanced antibacterial activity than the ligand against various bacterial strains. The BSA binding activity of the complexes shows that the affinity for binding is greater towards copper complex. The cytotoxicity of the ligand and its complexes are tested on HT29 colon cancer cells using MTT assay.

Keywords: Schiff base, Microwave synthesis, Antibacterial studies, BSA, Cytotoxicity

Bioinorganic complexes play vibrant role in the human physiological system. Among various type of metal complexes, Schiff bases and their corresponding metal complexes have been studied with great enthusiasm by inorganic chemists. Even though innumerable number of papers have been reported on Schiff base complexes, for decades, the researchers are still fascinated by the immense diversity of their applications. The facile synthetic methods, easy availability and electronic properties are the motivation for the extensive research of Schiff base complexes.

The nitrogen, sulphur and oxygen donor atoms available in Schiff bases can make this class of compounds very efficient catalysts in different organic reactions like oxidation, reduction, bond formation, hydrolysis etc[1-4]. By thoughtfully inserting electron withdrawing or donating substituent, the electronic properties of the Schiff bases can be fine-tuned according to our need. Because of this interesting option, they find very attractive and diverse applications like antimicrobial agents[5], sensor materials[6], pharmacological and electrochemical agents[7]. Due to the existence of azomethine group, and other hetero atoms like sulphur in the structure, Schiff bases together with their complexes are reported to exhibit significant bioactivity[8].

Proteins are the most profuse macromolecules in cells and are crucial in maintaining normal cell functions. Bovine serum albumin (BSA), being the major component in blood plasma, plays a significant role in the transport as well as metabolism of various endogenous and exogenous compounds. Since the serum albumin is found to be non-antigenic and biodegradable, and also readily available, the albumin is used as a biomaterial, in drug delivery and as novel hydrophilic carrier material. Recently, their conjugation with Schiff base is proved to improve their bioactivity effectively[9]. Binding of the Schiff base metal complexes with this carrier protein opens the gateway for drug-protein binding which is found to greatly influence its absorption, transport and metabolism properties of usual drugs in vertebrates.

Cancer has been deliberated to be one of the most fatal diseases in this present era. Recently, investigations on the cytotoxicity of Schiff bases

along with their complexes are increasing exponentially. Observations point to the fact that, the anticancer property of Schiff bases is significantly increased by coordination to metal ions[10-14]. Chelation theory can explain this enhanced bioactivity accounted lipophilic and penetration ability of complexes into the lipid membrane[15]. In rare cases, the ligands were found to show higher bioactivity than their complexes[16]. Drugs which are used in the cancer treatment follow different mechanism[17]. However, the results are not very encouraging, because they harm the healthy cells also. Hence, it is imperative to discover new anticancer agents with safe and enhanced activity to fight this dreaded disease.

As mentioned earlier, Schiff base complexes have been extensively studied for various applications. In recent years, we have studied the catalytic applications of some Schiff base complexes[18-20]. We have also established that the electron beam irradiation significantly enhances the catalytic efficacy of Schiff base complexes[21,22]. The interesting electrochemical properties of Schiff base complexes have been reported by us[23]. The Schiff base complexes have been found to be very good antimicrobials[24-26]. We have confirmed the excellent DNA/BSA binding abilities of various Schiff base complexes[27-29]. The Schiff base complexes also exhibit good chemical nuclease activity[25,26].

From intense literature survey, and with the background of our previous publications, we thought the sulphur donor Schiff base complexes can reveal very good biological applications. Hence, in this work, we have synthesized, characterized and investigated the bioactivity of a novel *SNSN* donor Schiff base, derived from thiophene-2-carbaldehyde and pyridine substituted thiosemicarbazide, and its complexes with Co(II), Ni(II), Cu(II) and Zn(II) metal ions.

Materials and Methods

Thiophene-2-carboxaldehyde and 4-(pyridin-2-yl)-thiosemicarbazide were purchased in pure form, from Sigma Aldrich and were used as such. The metal salts used in the present study, cobalt(II) chloridehexahydrate, nickel(II) chloride hexahydrate, copper(II) chloride dihydrate and zinc(II) chloride were obtained from Loba Chemie. Tris-buffer was obtained from HIMEDIA and BSA was procured from Aldrich.

Synthesis of ligand and its complexes

Equimolar quantities of thiophene-2-carbaldehyde and4-(pyridin-2-yl)-thiosemicarbazide were mixed thoroughly with minimum quatity of ethanol (5 mL) in a clean dry beaker. It was then heated in a microwave oven at 100 W power for 10 min. The yellow colour Schiff base (L) formed was repeatedly washed with ether and dried *in vacuo*. Equimolar mixture of the ligand (L) and the corresponding metal salts were mixed with 3 mL of methanol and reacted in a microwave oven for 10 min. The synthesis of Co(II) complex was carried out in nitrogen atmosphere. The newly formed Co(II), Ni(II), Cu(II) and Zn(II) complexes of the Schiff base **L** were washed repeatedly with water and dried. Schematic representation of the Schiff Base ligand and its complexes are shown in Scheme 1.

Characterisation techniques

The ^{1}H and ^{13}C NMR spectrum of Schiff base **L** was recorded on a JEOL GSX-400 spectrometer taking $CDCl_3$ as solvent at normal room temperature. The mass spectrum (EI) was detected using JEOL D-300 mass spectrometer. The infrared spectra of all the samples were obtained using JASCO/FT-IR 410 spectrometer in the wavenumber range of 4000-400 cm^{-1}. Electronic spectra in the range of 200-800 nm were recorded using Perkin Elmer Lambda-35 UV-visible spectrophotometer using DMSO as

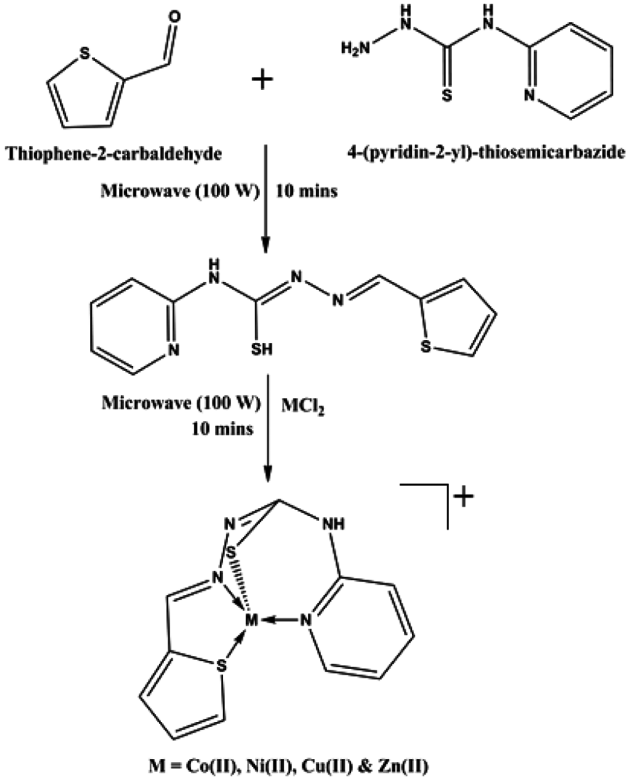

Scheme 1 — Schematic representation of the Schiff Base ligand and its complexes

solvent. The molar conductivities of the complexes were obtained in ~10^{-3} M DMSO solution using a coronation digital conductivity meter. Magnetic susceptibility measurements were obtained on Hertz SG8-5HJ model Gouy magnetic balance using $CuSO_4.5H_2O$ as the calibrant. The emission spectra were detected on a Perkin Elmer LS-45 fluorescence spectrophotometer. TG/DTG analyses of the complexes were obtained from SIINT 6300, under a dynamic N_2 atmosphere in the 20–800 °C temperature range at a heating rate of 10 °C min^{-1}. Powder XRD determinations of the compounds were made using an X-ray diffractometer (XPERT PRO PANalytical, Netherland). The patterns were run with Cu Kα radiation (λ = 0.1545 nm) with a generator at 40 kV and 40 mA at 25 °C temperature. The diffracting angle (2h) range for XRD spectroscopy from 10° to 80° was attained with a rate of 2° min^{-1}.

Antibacterial studies

Antimicrobial activities of the ligand along with its complexes were studied against three bacterial strains i.e., *Escherichia coli, Klebsiella pneumonia* and *Salmonella typhi* using agar well diffusion method by sterilizing the Mueller Hinton agar media. After solidification, the wells on the Mueller Hinton agar were cut bya cork borer. The bacterial pathogens to be tested were wiped on the surface of Mueller Hinton agar plates. The cut pieces of thin film of samples were placed on the well. All the plates were incubated at 37 °C for 24 h, and then the zone of inhibition formed was measured in millimeters.

BSA binding studies

The interaction of all the metal complexes with Bovine serum albumin (BSA) were studied in a buffer medium of 5 mM Tris-HCl/50 mM NaCl maintained at a pH of 7.5. The fluorescence spectral titrations were conducted at varied concentration of the complexes while keeping the BSA concentration as constant. The emission spectra of the system were recorded between the wavelength range of 250–450 nm upon excitation at 280 nm[30]. The absorption spectra for a fixed concentration of both BSA and metal complexes were recorded within 250–310 nm of wavelength.

Anticancer studies

Culturing of cells

HT29 cells were bought from the National Centre for Cell Sciences (NCCS), Pune, India, and were grown in a solution of minimum essential medium (MEM) containing 10% of 100 IU/mL FBS, penicillin 100 mg/mL and streptomycin 20 mg/mL. The cells were preserved as single layers in 25 cm^2 plastic tissue culture flasks maintaining the temperature at 310 K at humid conditions bearing 5% CO_2. The cells were reported to be multiplied in the culture, which were used all through theexperiments.

MTT assay

MTT assay was performed to probe the anticancer activity of L, [CoL]Cl, [NiL]Cl, [CuL]Cl and [ZnL]Cl on HT29 cancer cells. 200 µL of suspension of HT29 cells ($1x10^5$ cell/mL) was added to each well of 96 well micro titer plates and subjected to incubation for 24 h. When the incubation period is over, varying concentrations of the samples (10, 20, 30, 40 and 50 µg/mL) were added to the cells. 20 µL of MTT dye was added to each well after 24 h time of incubation. The media containing MTT dye solution was removed after 4 h. To each well, 200 µL of DMSO was added to dissolve the formazan crystals formed. The absorbance was measured at 570 nm, by a microplate reader spectrophotometer. This measurement was repeated three times (in triplicate) in three different days. Percentage cell toxicity values were calculated using the following equation,

$$\text{Cell viability (\%)} = \frac{\text{Sample absorbance}}{\text{Control absorbance}} \times 100 \qquad ...(1)$$

Results and Discussion

NMR spectral studies

In the ^{1}H NMR spectrum of the ligand **L** (Fig. 1a) the singlet appearing at 2.51 ppm corresponds to thioenol hydrogen of thiosemicarbazide moiety. The peak at 3.41 ppm is due to C-NH proton. The singlet appears at 7.56 ppm corresponds to the most important azomethine group. The signals in the range of 7.1-8.2 ppm arise as a result of aromatic protons of the ligand. The ^{13}C NMR spectrum of the ligand **L** (Fig. 1b) shows signals at δ 109.77, 114.97, 140.68 and 147.99 and 159.11 corresponds to aromatic carbons of thiosemicarbazide moiety. The signal at δ 126.12 corresponds to the azomethine carbon. The signal at δ 126.70, 127.85 and 146.93 corresponds to aromatic carbons of thiophene moiety. The signal obtained at δ183.42 corresponds to –C=S carbon. The ^{1}H NMR spectrum of [ZnL]Cl is provided in Fig. 1c. The NMR spectrum of the Zn(II) complex is very similar to that of the **L**, but for few changes. The signal due to thioenol proton, at δ 2.51, has disappeared. This confirms the coordination of the thioenolic sulphur with Zn(II) through covalent bond.

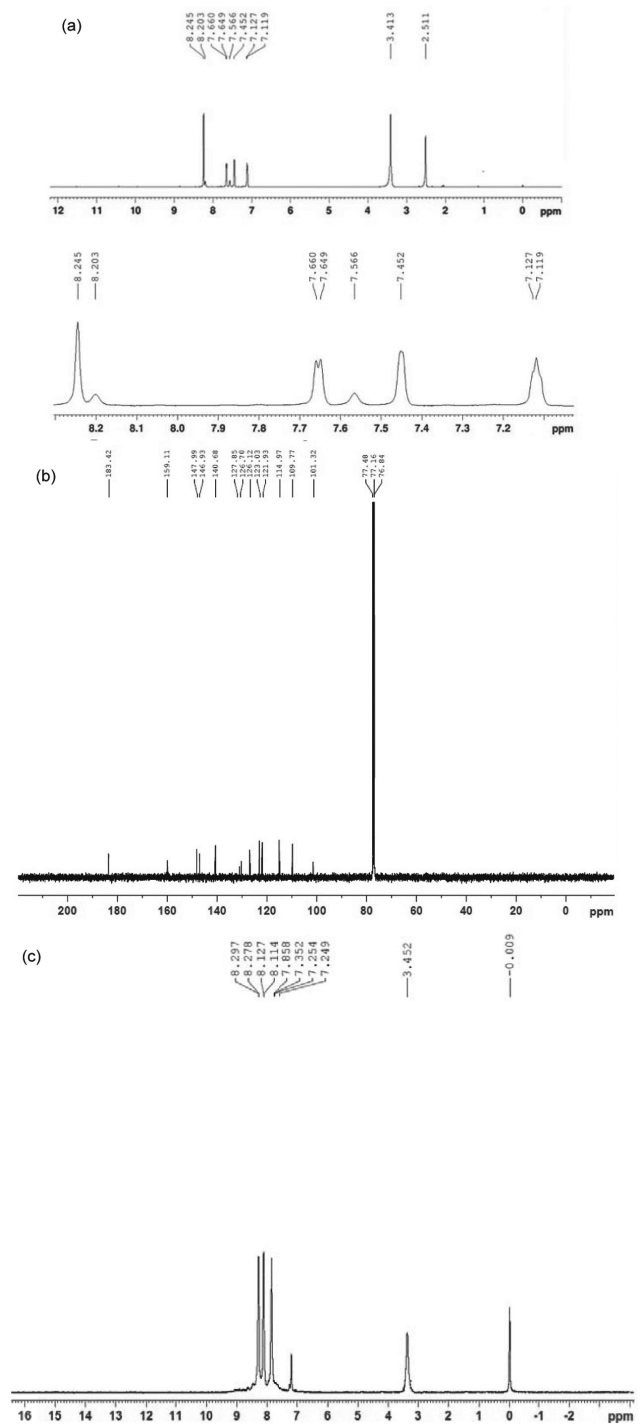

Fig. 1 — (a) ^{1}H, (b) ^{13}C NMR spectrum of Schiff base ligand **L** and (c) ^{1}H NMR spectrum of complex [ZnL]Cl

The intensity of the signal due to imino proton, at ~ 7.54, has been considerably reduced, because of the coordination of imino nitrogen to Zn(II), which in turn reduces the electron density of the proton significantly. The changes in the positions and intensities of all other protons are insignificant.

EI Mass spectrum

The EI mass spectrum of the ligand (Fig. 2) shows the molecular ion (M^+) peak at m/z = 262.12 corresponding to the molecular weight of the ligand. The peaks at m/z = 182.12, 154.21, 126.16, 98.12, 74.12 and 64.53 corresponds to various fragments $C_7H_7N_4S$, $C_6H_5N_3S$, $C_5H_4N_2S$, C_5H_4S,C_4H_3S and C_4H_4N, respectively, which in turn concurs with the proposed structure the Schiff base.

FTIR spectra

The FTIR spectrum of the **L** (Fig. 3a) exhibits a band at 1674 cm^{-1}, due to the imino (CH=N) stretching confirming the Schiff base formation[31]. The C-N stretching of pyridine is observed at 1479 cm^{-1}. The C-S stretching of thiophene is found at 1173 cm^{-1} and the C-S stretching of thioenol appears at 1143 cm^{-1}. The FTIR spectra clearly confirm the formation of the Schiff base L, with the expected structure. It also suggests that the thiocarbonyl group may be partly present in its enolic form.

In the FTIR spectra of the complexes (Fig. 3(b-e)), the band corresponding to the azomethine group in **L** (1674 cm^{-1}) is shifted towards lower wavenumber region[28] which approves the coordination of the imino nitrogen atom to the corresponding metal ion forming stable complexes (Table 1). Similarly, in the complexes, the band for pyridine C-N stretching have been shifted to lower wavenumber which is also the case for thiophenyl C-S stretching and thioenol C-S frequency, confirming the effective coordination of ligand L to metal ions. The new bands arising in the region of 550 cm^{-1} is ascribed to the formation of M-N bonds[32,33]. The vibrational spectra of the complexes show that the ligand L is coordinated to the metal ions through imino and pyridine nitrogen atoms.

Electronic spectra, molar conductance and magnetic measurements

The electronic spectra of the complexes are provided in Fig. 4. In all the complexes, the high intense peak around 300 nm corresponds to π-π* transition[34]. The electronic spectrum of [CoL]Cl has only one d-d band in the visible region at 520 nm, due to $^{4}A_2(F) \rightarrow {}^{4}T_1(P)$ transition indicating sp^3 hybridized tetrahedral geometry. The d-d band for [NiL]Cl is observed at 510 nm, which is due to the $^{3}T_1(F) \rightarrow {}^{3}T_1(P)$ transition demonstrating tetrahedral geometry, with sp^3 hybridization. The spectrum of [CuL]Cl exhibits two less intense d-d bands centered at 525 nm and 700 nm due to $^{2}B_{1g} \rightarrow {}^{2}E_g$ and $^{2}B_{1g} \rightarrow {}^{2}B_{2g}$ transitions corresponding to dsp^2 hybridized

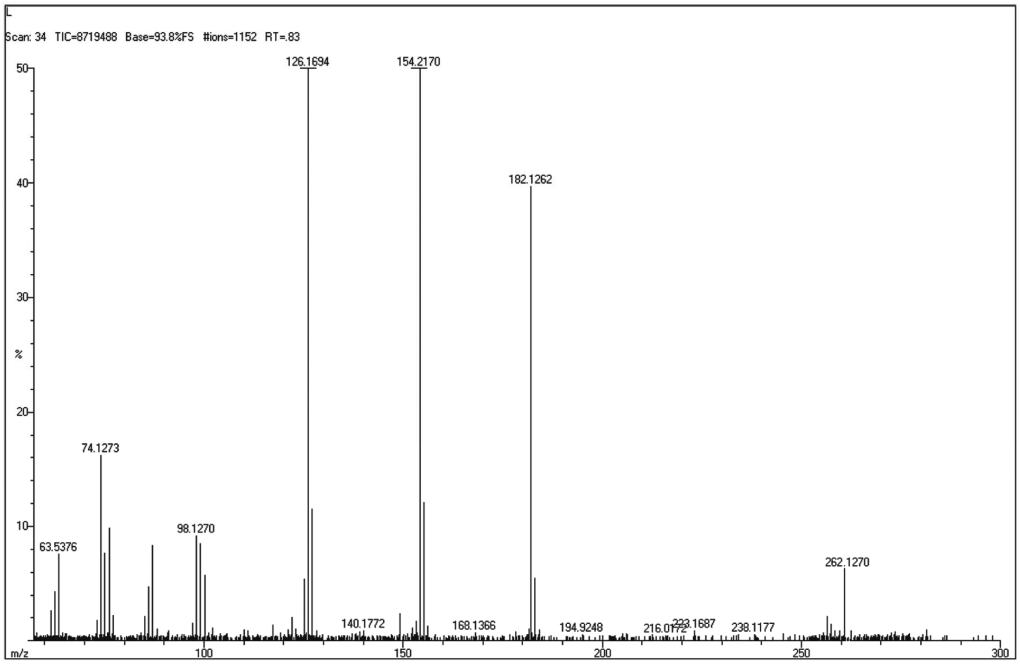

Fig. 2 — EI-Mass spectrum of Schiff base ligand **L**

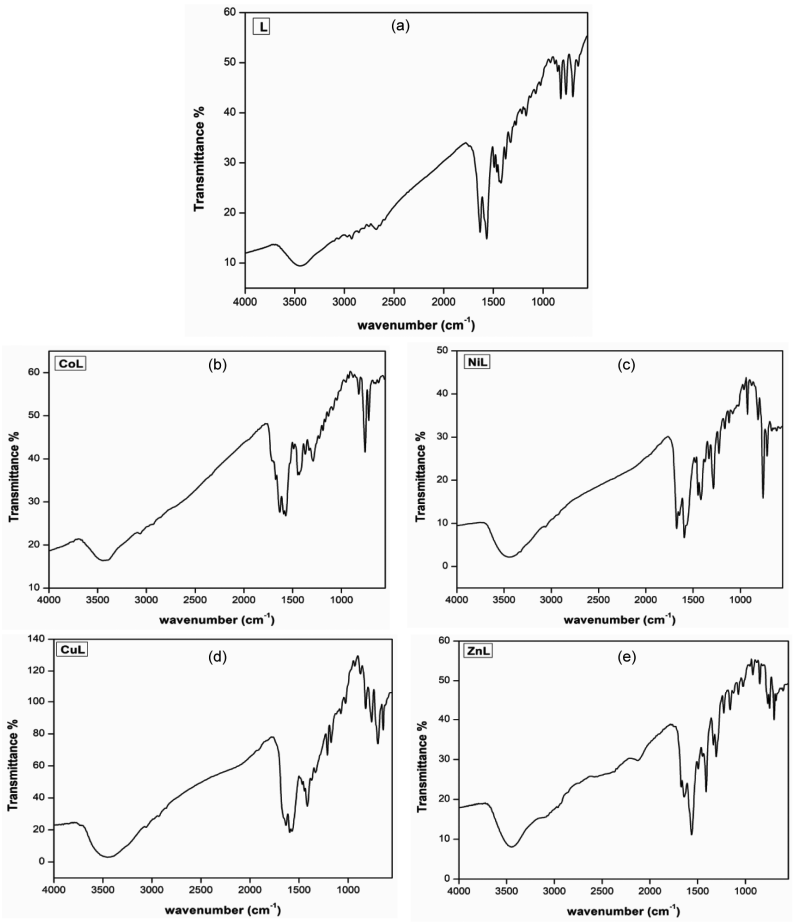

Fig. 3 — FTIR spectrum of (a) Schiff base ligand **L** and (b-e) of the complexes

Table 1 — FTIR frequencies of ligand and its complexes

Compounds	$\nu_{(CH=N)}$ (cm^{-1})	$\nu_{C-S(thiophene)}$ (cm^{-1})	$\nu_{C-S(thioenol)}$ (cm^{-1})	ν_{C-N} (cm^{-1})	ν_{M-S} (cm^{-1})	ν_{M-N} (cm^{-1})
L	1674	1172	1143	1479	-	-
[CoL]Cl	1632	1163	1131	1463	593	554
[NiL]Cl	1645	1165	1137	1458	598	558
[CuL]Cl	1627	1152	1129	1466	592	553
[ZnL]Cl	1623	1158	1136	1461	595	551

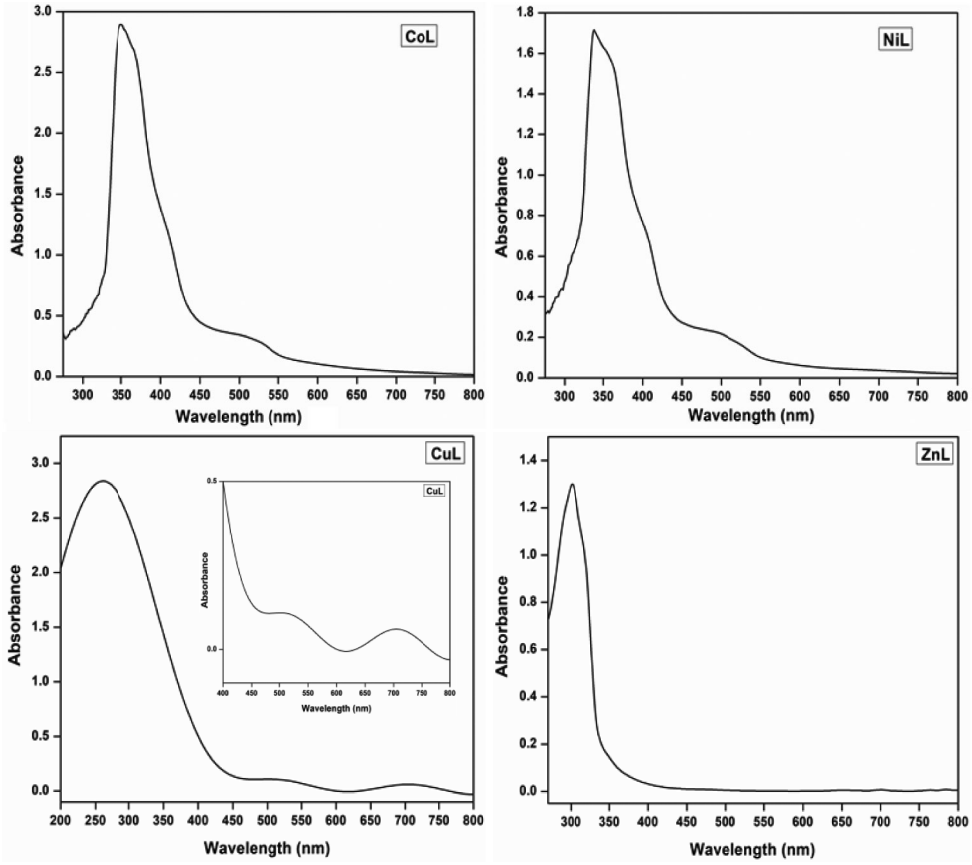

Fig. 4 — Electronic spectra of the complexes

square planar geometry[35,36]. [ZnL]Cl complex does not exhibit any d-d electronic transitions due to its completely filled d^{10} electronic configuration. However, four coordinate Zn(II) complexes, in general, would have tetrahedral geometry[37].

The molar conductance values of [CoL]Cl, [NiL]Cl, [CuL]Cl and [ZnL]Cl are 54, 54, 53 and 53 S mol^{-1} cm^2, respectively. These values of molar conductance suggest that the complexes are 1:1 electrolytic in nature. Hence, we can conclude that, the chloride ion is present outside the coordination sphere of unipositive cationic complex. This is confirmed by the positive silver nitrate test.

The [CoL]Cl complex has a magnetic moment of 4.48 B.M, which is well agreed with the reported value for tetrahedral Co(II) complex. Generally, square planar Ni(II) complexes are found to be diamagnetic whereas tetrahedral complexes possess magnetic moments in the range of 3.2–4.1 B.M. The present synthesized [NiL]Cl complex possess a magnetic moment value of 3.37 B.M at room temperature, which is consistent with tetrahedral geometry[38,39]. The magnetic moment value of the [CuL]Cl complex is 1.87 B.M., indicating that the complex is monomeric and paramagnetic. Hence, the [CuL]Cl complex can be assigned square planar geometry of dsp^2 hybridization[40].

EPR spectrum

The X-band EPR spectrum of [CuL]Cl at a temperature of liquid nitrogen (LNT) is shown in Fig. 5. The hyperfine splitting structure acquired

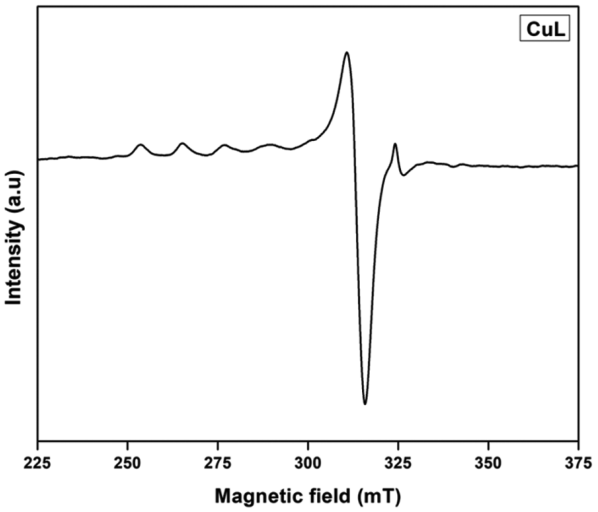

Fig. 5 — EPR spectrum of the complex [CuL]Cl

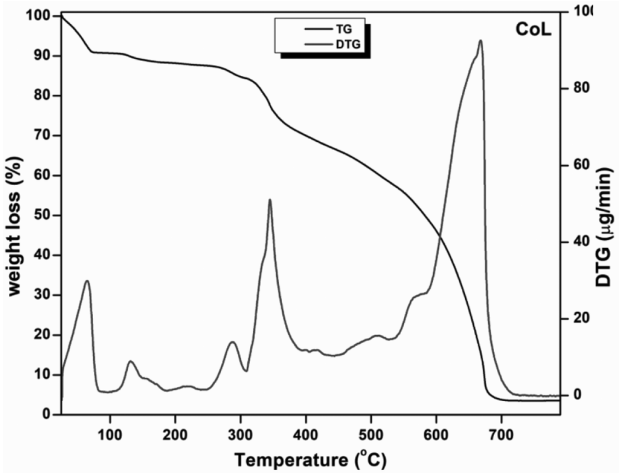

Fig. 6 — TG/DTG curves for the complex [CoL]Cl

agrees to the square planar geometry of the complex. The spectrum shows four lines due to hyperfine splitting having a nuclear spin value of 3/2. i.e., four low intense well resolved peaks at low-field region and one intense peak in high-field region as a result of coupling of the unpaired electron with the nuclear spin of Cu(II)[41]. The $g_{\|}$ and $g_{\perp}$ values are found to be 2.242 and 2.158, respectively, which follows the trend of $g_{\|} > g_{\perp} > 2.0023$ showing that the unpaired electron is in the $d_{x^2-y^2}$ orbital having $^2B_{1g}$ as the ground state[42].

Thermal studies

TG/DTG measurements of the complexes were studied in the temperature range of 25-800 °C (Fig. 6, S1-S3, Supplementary Data). The thermograms of the complexes show weight loss upto 100 °C, accompanied by the removal of lattice water molecules

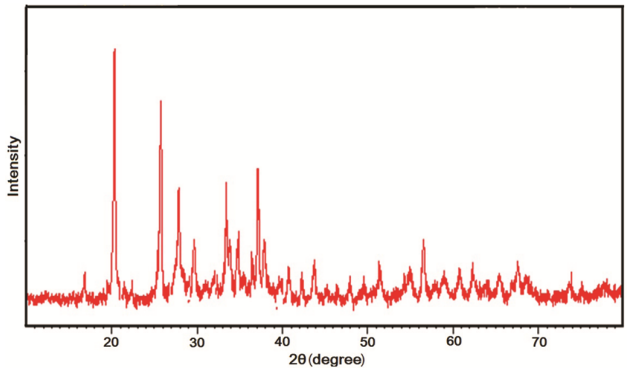

Fig. 7 — Powder X-ray diffractogram of the complex [CoL]Cl

and chloride ions present outside the coordination sphere of the complexes. In [CoL]Cl, decomposition at 370 °C corresponding to a weight loss of 20% is due to the partial decomposition of coordinated ligand. The next step of the thermal degradation that occurs between 530–650 °C (~36% weight loss) corresponds to the removal of remaining organic ligand moiety leaving the metal oxide residue. However, in [NiL]Cl weight loss at 350 °C is due to partial decomposition of ligand and a major degradation at 450-550 °C is due to complete decomposition of organic ligand moiety leaving behind the metal oxide residue. Thermal decomposition curve of [CuL]Cl shows weight loss of 80% at 350 °C corresponding to the decomposition of major part of the coordinated ligand. The next step of the thermal degradation that occurs between 450 °C (~10% weight loss) corresponds to the removal of remaining organic ligand moiety leaving the metal oxide residue. In [ZnL]Cl, thermal decomposition occurring at 300 °C corresponding to a weight loss of 32% is due to the partial decomposition of coordinated ligand. The next step of the thermal degradation occurring between 520–680 °C (~40% weight loss) corresponds to the removal of remaining organic ligand moiety leaving the metal oxide residue.

Powder X-ray diffraction

The XRD data of [CoL]Cl complex (Fig. 7) is recorded at room temperature in the range of 0-80°. Several peaks with high intensities were detected from XRD. These peaks can be listed as follows; 20.45, 25.92, 28.11, 33.64, 37.53, 56.84. The highest intensity was found at the peak of 20.45°. XRD measurement confirmed that this complex is a cystalline solid. The average grain size values of the [CoL]Cl complex was obtained from Debye-Scherrer equation and is found to be 54 nm.

Table 2 — Antimicrobial activity of the compounds treated against bacterial pathogens

Test organisms	Zone of inhibition (diameter) in mm						
	L	[CoL]Cl	[NiL]Cl	[CuL]Cl	[ZnL]Cl	Amickacin	Control Sample
E.coli	15	17	22	23	19	23	NZ
Klebseilasp	13	15	15	18	20	25	NZ
Salmonella sp	12	17	16	19	21	21	NZ

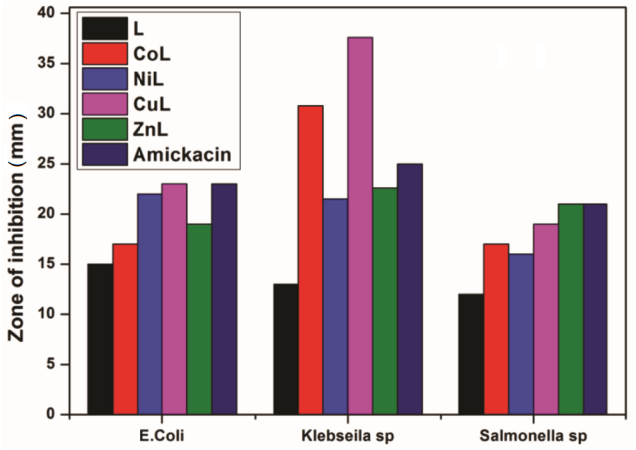

Fig .8 — *In vitro* antimicrobial activity of the ligand and their complexes

Antibacterial activities

Antimicrobial activities of L and its complexes have been tested against the bacterial species *Escherichia coli, Klebsiella pneumonia* and *Salmonella typhi.* The results of the antibacterial activities are summarized in Table 2, and illustrated in Fig. 8 and Fig. S4 in Supplementary Data. In the present study, the antibacterial activity of the ligand and its complexes indicate that the complexes acquire higher activity compared to that of ligand. However, the bioactivity of the compound varies with metal ions. On complexation with the metal ions the antibacterial activity is considerably increased. This increased activity of the complexes than their corresponding ligand could be explained on account of Tweedy's chelation theory[43]. Chelation can reduce the metal ion polarity by the partial sharing of its positive charge with the donor atoms from ligand along with delocalization of π-electrons on the chelate ring. The cell wall and membranes are found to be made up of lipids and polysaccharides which are preferable sites for metal ion interaction. Also the cell walls contain many ligands viz., phosphates, carbonyl and cystenyl groups for maintaining the cell membrane integrity by acting as a barrier towards diffusion and providing suitable sites for binding. The interaction between the metal ion and the lipid molecule leads to the damage of the cell permeability thereby causing intrusion in the routine cell processes[44].

BSA binding studies

Fluorescence spectroscopy

The intrinsic fluorescence of BSA appearing at 340 nm caused by the tryptophan 212 moiety[45] is found to be quenched on addition of varying concentrations of metal complexes (Fig. 9a, S5-S7). This process of quenching occurs *via* a mode of either static or dynamic. The dynamic quenching is the result of molecular collisions whereas static quenching is accounted by ground-state complex formation between the protein molecule and quencher i.e., complexes. The mechanism behind this quenching process can be obtained from Stern-Volmer equation as follows[46].

$$\frac{F_0}{F} = 1 + K_{SV}[Q] = 1 + K_q\tau_0[Q] \quad \text{... (2)}$$

The F_0 and F represent the emission maxima without and presence of quencher molecules, respectively. The Stern-Volmer quenching constant is K_{sv} with the quencher concentration [Q] and τ_0 being the mean life time of protein which is 10^{-8} s for BSA[47]. K_q is denoted to be the quenching rate constant of the protein and is obtained from K_{sv}/τ_0. The K_{sv} is the slope value of the linear fit obtained by plotting F_0/F *vs* [Q] (inset of Fig. 9a, S11-S13). The K_{sv} and K_q values for[CoL]Cl, [NiL]Cl, [CuL]Cl&[ZnL]Cl complexes provided in Table 3. Since the K_q values obtained were greater than 2.0 x 10^{10} L mol^{-1} s^{-1} it could be concluded that the mechanism accounted for quenching was static mode. The aforesaid value is the maximum scattering collision quenching constant obtained for various quenchers on account of dynamic quenching[48]. This shows that the BSA quenching by the synthesized complexes is caused by ground-state complex formation between BSA and complexes.

Absorption spectroscopy

The ground state complex formed between the BSA protein and the metal complexes can be further validated by UV-visible absorption spectra recorded in the range of 200–350 nm. The absorption spectra of BSA after addition of metal complex is found to undergo a

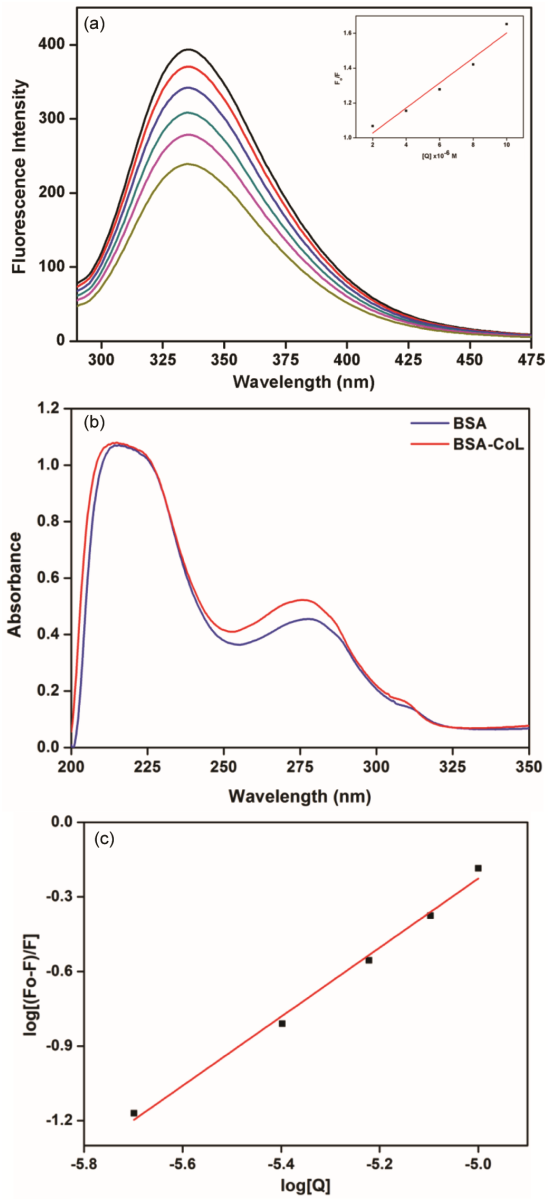

Fig. 9 — (a) Emission spectra of BSA in the presence of various concentrations of [CoL]Cl complex in DMSO (T=298K), c(BSA)=2.0 × 10-6 mol L^{-1}, c[CoL]Cl = 2, 4, 6, 8, 10 × 10^{-6} mol L^{-1}. Inset: Stern-Volmer plot for quenching of BSA by [CoL]Cl complex, (b) UV-visible absorption spectra of BSA and BSA-CoL solutions: c(BSA) = c[CoL]Cl = 2 × 10^{-6} mol L^{-1} and (c) Double logarithm plot for BSA-[CoL]Cl

bathochromic shift (Fig 9b, S8-S10) confirming the static mode of quenching mechanism[49].

Analysis of binding constants and binding sites

The extent of binding of metal complexes with BSA is obtained by calculating the binding constants (K_b) and the number of binding sites (n) using the following equation[50],

Table 3 — K_{sv} and K_q values of the complexes

Complexes	K_{sv}(× 10^4 L mol^{-1})	K_q(× 10^{12} L mol^{-1} s^{-1})
[CoL]Cl	4.18	4.18
[NiL]Cl	4.25	4.25
[CuL]Cl	4.35	4.35
[ZnL]Cl	4.29	4.29

Table 4 — Binding constant (K_b) and Binding site (n) values of the complexes

Complexes	Binding constant (× 10^4 Lmol^{-1}) K_b	Binding site n
[CoL]Cl	5.36	1.07
[NiL]Cl	5.48	1.02
[CuL]Cl	5.86	1.11
[ZnL]Cl	5.63	1.09

$$\log\left(\frac{F_0-F}{F}\right) = \log K_b + n\log[Q] \quad \ldots (3)$$

Where, K_b and n values (Table 4) are the intercepts and slopes obtained from the linear fits on plotting log F_0-F/F *vs* log [Q] at 298 K (Fig. 9c, S11-S13) for the metal complexes, respectively. The binding site values are approximated to 1 revealing the presence of only one binding site in BSA where the complexes could bind. Among the two tryptophan residues in present in BSA molecule i.e., Trp-134 in sub-domain IA and Trp-212 in hydrophobic sub-domain IIA, the binding of drug molecules to sub-domain IIA result in conformational changes[51]. This shows that the complexes could bind with Trp-212 in sub-domain IIA.

Anticancer activities

MTT assay on HT29 cell lines was performed in order to find the relative cell viability after treating with different concentrations of the metal complexes. This studies show the maximum concentration at which the cell mortality is higher for cancer cell lines under study. The cytotoxic effects induced by metal complexes at different concentrations (10, 20, 30, 40, 50 µg/mL) in HT29 cells is shown in Fig. 10. It has been observed that the percentage cell toxicity increases with increase in metal ions concentration and it was found to be maximum at the concentration of 50 µg/mL (Table 5). It has been observed that [CuL]Cl complex exhibits higher anticancer activity than the ligandas well as other synthesised metal complexes. The higher cytotoxicity of [CuL]Cl can be well explained by its higher BSA binding ability.

Comparison of biological activity

Recently Jeslin and coworkers[52] have studied the biological activities of Ni(II), Cu(II) and Zn(II)

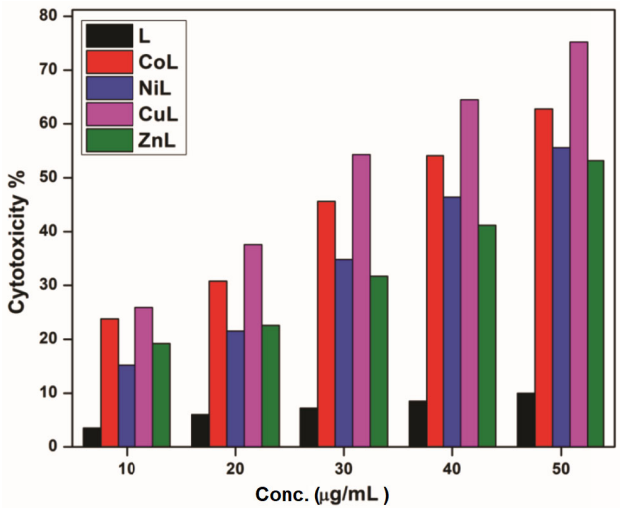

Fig. 10 — Cytotoxicity of HT29 cell line determined by MTT assay challenged with increasing concentrations (10, 20, 30, 40, 50 µg/mL) of the complexes after 24 h

Table 5 — Cytotoxicity of the complexes against HT29 cell line

Complexes	10 µg/mL	20 µg/mL	30 µg/mL	40 µg/mL	50 µg/mL
L	3.5	6	7.2	8.5	10
[CoL]Cl	23.8	30.8	45.6	54.1	62.8
[NiL]Cl	15.2	21.5	34.8	46.4	55.6
[CuL]Cl	25.9	37.6	54.3	64.5	75.2
[ZnL]Cl	19.2	22.6	31.7	41.2	53.2

Table 6 — Zone inhibition of Schiff base complexes against bacteria – Comparative data

Complex	E.coli	Klebsiela sp
Ni(II)-o-Van-1,3DAP[53]	6.4	5.8
Cu(II)-o-Van-1,3DAP[53]	10.5	8.3
Zn(II)-o-Van-1,3DAP[53]	9.7	8.6
Cu(II)-Acenaphthene quinine-methionine[25]	15	16
Ni(II)-Cumal-4-AAP[24]	-	12.5
Cu(II)-Cumal-4-AAP[24]	12.5	12.2
Zn(II)-Cumal-4-AAP[24]	10.2	10.2

complexes, with Schiff base derived from o-vaniline and 1,3 diamino propane. The binding constants of Ni(II), Cu(II) and Zn(II) with CT DNA are 1.43, 0.87 and 3.08 (10^4), respectively. Previously we have reported[53] the binding constant of Mn(III) and Fe(III) with the Schiff base of phenanthroquinone and tyrosin as 4.37 and 4.66 (10^4), with BSA. Similarly, the binding constant values of the complexes Mn(III)-PQ-Phe and Fe(III)-PQ-Phe with BSA are 4.67 and 4.18 (10^4), respectively.[27] However, in this present study the binding abilities of the Schiff base complexes with BSA are much higher, namely 5.48, 5.86 and 5.63 (10^4) for [NiL]Cl, [CuL]Cl and [ZnL]Cl, respectively. Hence it is evident the new SNSN donor Schiff base complexes exhibit distinctly higher binding affinities with BSA. Likewise, the Schiff base complexes of the present study, obviously demonstrate higher efficiency against the bacteria, as illustrated in the Table 6.

Conclusions

A novel *SNSN*donor based Schiff base ligand involving thiophen-2-carbaldehyde and 4-(pyridin-2-yl)-thiosemicarbazide along with its Co(II), Ni(II), Cu(II) and Zn(II) metal complexes were synthesized and characterized using several analytical and spectroscopic tools. The antibacterial studies reveal that the complexes exhibit greater activity than that of the ligand. The BSA binding experiments of the complexes shows static mode of quenching which were further confirmed from absorption experiments. The binding constant was found to be greater for [CuL]Cl and the number of binding sites were approximated one for all the complexes into hydrophobic sub domain IIA of BSA. The anticancer activity of the complexes against HT29 cell lines reveal the greater cytotoxic activity of [CuL]Cl than ligand and other complexes.

Supplementary Data

Supplementary data associated with this article are available in the electronic form at http://nopr.niscair.res.in/jinfo/ijca/IJCA_60A(11)1416-1426_SupplData.pdf.

References

1 Şahal H, Canpolat E, Kaya M & Kara N, *J Chem Soc Pakistan*, 37 (2015) 245.
2 Ahmad S N, Bahron H, Tajuddin A M & Abd, S A I A S, *Jurnal Teknologi*, 80 (2018).
3 Bahron H, Khaidir S S, Tajuddin A M, Ramasamy K & Yamin B M, *Polyhedron*, 161 (2019) 84.
4 Sutradhar M, Alegria E C, Guedes da Silva M F C, Martins L M & Pombeiro A J, *Molecules*, 21 (2016) 425.
5 Zaltariov M F, Cazacu M, Avadanei M, Shova S, Balan M, Vornicu N & Varganici C D, *Polyhedron*, 100 (2015) 121.
6 BartocciS, Sabaté F, Bosque R, Keymeulen F, Bartik K, Rodríguez L & Dalla Cort A, *Dyes Pigm*, 135 (2016) 94.
7 Shabbir M, Ahmad I, Ismail H, Ahmed S, McKee V, Akhter Z & Mirza B, *Polyhedron*, 133 (2017) 270.
8 Tarafder M T H, Jin K T, Crouse K A, Ali A M, Yamin B M & Fun H K, *Polyhedron*, 21 (2002) 2547.
9 Rasmussen D D, Ishizuka B, Quigley M E & Yen S S C, *J Clin Endocrinol Metab*, 57 (1983) 760.
10 Alsalme A, Laeeq S, Dwivedi S, Khan M S, Al Farhan K, Musarrat J & Khan R A, *Spectrochim Acta A*, 163 (2016) 1.
11 Hosseini-Yazdi S A, Mirzaahmadi A, Khandar A A, Eigner V, Dušek M, Mahdavi M & White J, *Polyhedron*, 124 (2017) 156.
12 Naureen B, Miana G A, Shahid K, Asghar M, Tanveer S & Sarwar A, *J Mol Struct*, 1231 (2021) 129946.

13 Zishen W, Ziqi G & Zhenhuan Y, *Synth React Inorg Met Org Chem*, 20 (1990) 335.
14 Thamilarasan V, Sengottuvelan N, Sudha A, Srinivasan P & Chakkaravarthi G, *J Photochem Photobiol B*, 162 (2016) 558.
15 Aly H M, Moustafa M E, Nassar M Y & Abdelrahman E A, *J Mol Struct*, 1086 (2015) 223.
16 Tajuddin A M, Ramasamy K, Yamin B M, Alharthi A I & Bahron H, *Arab J Chem*, 10 (2017) 769.
17 Kumar P, Narasimhan B, Ramasamy K, Mani V, Kumar Mishra R & Bakar Abdul Majeed A, *Curr Top Med Chem*, 15(2015) 1050.
18 Antony R, Theodore David Manickam S, Kollu P, Chandrasekar P V, KaruppasamyK & Balakumar S, *RSC Adv*, 4 (2014) 24820.
19 Antony R, Theodore David Manickam S, Kollu P, Chandrasekar P V, Karuppasamy K & Balakumar S, *RSC Adv*, 4 (2014) 42816.
20 Antony R, Theodore David Manickam S, Saravanan K, Karuppasamy K & Balakumar S, *J Mol Struct*, 1050 (2013) 53.
21 Antony R, Suja Pon Mini P S, Theodore David Manickam S, Ganesh Sanjeev, LiviuMitu & Balakumar S, *Spectrochim Acta A*, 149 (2015) 550.
22 Antony R, Theodore David Manickam S, Karuppasamy K, Ganesh Sanjeev, Balakumar S, *SpectrochimActa A*, 124 (2014) 178.
23 SujaPon Mini P S, Antony R, Theodore David Manickam S, Thanikaikarasan S, Subramanian R, Balakumar S, Mahalingam T, Sergio Saldana & Luis Ixtlilco, *J. New Mat Electrochem Systems*, 17 (2014) 179.
24 Biju Bennie R, Theodore David S, Sivasakthi M, Daniel Abraham S, Joel C & Antony R, *Chem Sci Trans*, 3 (2014) 805.
25 MagalaSathyasheeli S, Theodore David S, MythiliC V & SujaPon Mini P S, *Der Pharm Chem*, 8 (2016), 312.
26 Theodore David S, & Sivasankaran Nair M, *Int J Appl Chem*, 7 (2011) 159.
27 Biju Bennie R, Joel C, Daniel Abraham S, IyyamPillai S & Theodore D Manickam S, *Acta Chim Slov*, 66 (2019)196.
28 Joel C, Biju Bennie R, Daniel Abraham S, Iyyam Pillai S & Theodore David S, *Appl Organomet Chem*, 32 (2018) e4516.
29 Biju Bennie R, Joel C, Daniel Abraham S, Theodore David S & IyyamPillai S, *Der Pharm Lett*, 8 (2016) 260.
30 Suryawanshi V D, Walekar L S, Gore A H, Anbhule P V & Kolekar G B, *J Pharm Anal*, 6 (2016) 56.
31 Warad I, Suboh H, Al-Zaqri N, Alsalme A, Alharthi F A, Aljohani M M & Zarrouk A, *RSC Adv*, 10 (2020) 21806.
32 Shakir M, Azam M, Parveen S, Khan A U & Firdaus F, *Spectrochim Acta A*, 71 (2009) 1851.
33 Baruah J M, Kalita S & Narayan J, *Int Nano Lett*, 9(2019) 149.
34 Devi R, BoddulaR, Singh K, Kumar S & Vaidyanathan S, *J Inf Disp*, 22 (2021) 137.
35 Aziz A & Lal R A, *Arab J Chem*, 10 (2017) 5901.
36 RaoT S, Reddy K L & LingaiahP,*Proc Indian Acad Sci*, 100 (1988) 363.
37 Temel H, İlhan S, Şekerci, M & Ziyadanoğullari R, *Spectrosc Lett*, 35 (2002) 219.
38 Cotton F A, Wilkinson G, Murillo C A, Bochmann M & Grimes R, *Advanced Inorganic Chemistry,* New York: Wiley 1988, p. 1455.
39 Banerjea D, *Coordination Chemistry*, Tata McGraw-Hill Pub., New Delhi, 1998.
40 Day M C & Selbin J, *Theoretical Inorganic Chemistry,* Litton Edu. Pub. Inc 1969.
41 Halevas E, Pekou A, Papi R, Mavroidi B, Hatzidimitriou A G, Zahariou G & Pantazaki A A, *J Inorg Biochem*, 208 (2020) 111083.
42 Chandrasekar T, Arunadevi A & Raman N, *J Coord Chem*, 74 (2021) 804.
43 Ramesh R & Maheswaran S,*J Inorg Biochem*, 96 (2003) 457.
44 Raman N, Sobha S & Mitu L, *J Saudi Chem Soc*, 17 (2013) 151.
45 Mondal S S, Jaiswal N, Bera P S, Tiwari R K, Behera JN, Chanda N & Saha T K, *Appl Organomet Chem*, 35(2021) e6026.
46 Ingle S A, Kate A N, Kumbhar A A, Khan A A, Rao S S & Gejji S P, *RSC Adv*, 5 (2015) 47476.
47 Aslam J, Lone I H, Ansari F, Aslam A, Aslam R & Akram M, *Spectrochim Acta A*, 250 (2021) 119350.
48 Wani T A, AlRabiah H, Bakheit A H, Kalam M A & Zargar S,*Chem Cent J*, 11 (2017) 134.
49 Xiang Y & Wu F, *Spectrochim Acta A*, 77 (2010) 430.
50 Singh N, Pagariya D, Jain S, Naik S & Kishore N, *J Biomol Struct Dyn*, 36 (2018) 2449.
51 Li L, Guo Q, Dong J, Xu T & Li J, *J Photochem Photobiol B*, 125 (2013) 56.
52 Jeslin KanagaInba P, Annaraj B, Thalamuthu S & Neelakantan M A, *Bioinorg Chem Appl*, 10 (2013) 1.
53 Biju Bennie R, Theodore David S, Joel C, Daniel Abraham S & IyyamPillai S, *Der Pharm Chem*, 6 (2014), 343.